Project no. 248992

Project acronym: NEUNEU

Project title: Artificial Wet Neuronal Networks from Compartmentalised Excitable Chemical Media

Small or medium-scale focused research project (STREP)

Deliverable 1.2 - Report about α-hemolysin facilitated BZ droplet excitation

Period covered: from 1.2.2010 to 29.2.2012 Date of preparation: 18.9.2009

Start date of project: 1.2.2010 Duration: 36 months

Project coordinator name: Dr. Peter Dittrich
Project coordinator organisation name: Friedrich Schiller University Jena

Microfluidics for linear microliter-volume droplet interface bilayer arrays

Philip H. King,[a] Hywel Morgan,[a] Maurits R. R. de Planque[a] and Klaus-Peter Zauner[b]*

[a] Centre for Hybrid Biodevices, Institute for Life Sciences, University of Southampton, Southampton, United Kingdom. Tel: +44 (0)2380 599307; E-mail: mdp@ecs.soton.ac.uk
[b] Agents, Interation and Complexity Group, Electronics and Computer Science, University of Southampton, Southampton, United Kingdom.

Abstract

Droplet interface bilayers (DIBs) have recently become popular as a simple and robust method for artificial lipid bilayer formation. Current methods of DIB formation often rely on manual pipetting and placement, or on dieletrophoretic chips that offer only limited numbers and formations of droplets. Microfluidic techniques are promising as a method to increase the scope of functional DIB networks towards greater complexity and automation of formation. Here we present a microfluidic device capable of large-volume droplet production and sequential linear trapping for large surface area bilayers that are stable over extended time periods. Droplets can be added to the array from separate droplet generators on-demand, allowing more complex linear arrays for the study of droplet-to-droplet translocation. The chips are fabricated using 3D-printing augmented soft lithography, allowing simple and rapid fabrication of moulds with high aspect ratio and 2.5D features. Finally, we probe the formation of DIBs in the array using the membrane-disrupting peptide melittin, and present a novel and simple colorimetric method for the tracking of bilayer formation using the staining of starch by potassium triiodide.

1. Introduction

The concept of droplet interface bilayers (DIBs) was first explored in the 1970s as a method for the production of artificial lipid bilayers.[1] However, the technique has only relatively recently attracted interest as an alternative the planar bilayer methods that have since become the convention.[2]

An outline of the formation of DIBs is shown in *Fig. 1*. Amphiphilic lipid is dissolved in either the oil (lipid-out) or the aqueous solution (lipid-in), where it forms energetically-favourable micelles. Introducing aqueous droplets into the oil causes the self-assembly of a lipid monolayer at the aqueous-oil interface, due to the polar nature of the aqueous medium. Where two droplets are bought into contact, a DIB can form at the droplet-to-droplet interface. Bilayers formed using this process been used in the literature for the analysis of protein pores,[3, 4] bilayer permeability,[5] and membrane stability on exposure to nanoparticles.[6]

The formation of DIBs can be achieved via a number of methods. The early research by L. Tsofina et al involved the production of aqueous, lipid-stabilised slugs that are brought together within an oil phase to form the bilayer.[1] This technique has subsequently been replicated on microfluidic chips,[7, 8] greatly miniaturising the process.

However, a major advantage of DIBs is the ability to produce networks of droplets. This network approach has been pioneered by the group of H. Bayley, who have demonstrated branching networks which show interface-mediated collective behaviour.[9, 10] The group has also recently demonstrated artificial multisomes that are inspired by the multicompartment nature of living cells.[11]

These networks are often formed using manual micro-pipetting. Although as a technique this is highly flexible, both in terms of droplet positioning and composition, it is not suitable for the next logical step for DIB networks: more complex, large-scale structures, which may be composed of hundreds or thousands of droplets. It is clear that any methods of generating such droplet structures need to be not only flexible but highly automated.

1.1 A microfluidic approach

Soft lithography has been the predominant technique for the prototyping of microfluidic devices in the last decade.[12] Moulds fabricated from patterned layers of photoresist are used to shape prepolymer poly(dimethylsiloxane) (PDMS).[13] The subsequently cured and demoulded PDMS structure can then be bonded to further PDMS, glass, or silicon to create internal microfluidic structures. This is normally achieved by treating the bonding surfaces with oxygen plasma.[14]

These techniques have become prevalent due to the flexibility and optical clarity of PDMS, the ease of bonding the chips, and the greater suitability of the process for prototyping in comparison to the micromachining of channels from glass or silicon. Soft lithography has allowed research laboratories without the cleanroom facilities required for micromachining to produce complex and functional microfluidic devices that can be tailored towards specific applications.

Where devices require the fabrication of very small features (<100 μm) the accuracy afforded by lithographic processes for mould production is still required. Furthermore, cleanrooms are still highly desirable for the fabrication of chips with such small features due to the risk of damage due to the adhesion of particles of dust or dirt that are present in unfiltered air. However, in many cases the use of photolithography is simply a hangover from the origins of microfluidics, where the first devices were produced using facilities developed for the production of silicon-based electronics. Photolithography is a highly manual, time-consuming process that is the rate-limiting step for the rapid production of microfluidic prototypes for research.

1.2 3D printing for PDMS mould production

The use of 3D printing (3DP) systems shows promise as a rapid, highly automated method for the production of moulds for soft lithography. Although the minimum feature size is not in the same range as photolithography, the resolution achievable is sufficient to produce devices with channels 200-300 μm in cross-section. Although 3DP has been used previously in this way,[15, 16] we have independently developed the process towards the production of large-volume droplet arrays, focussed on rapid turnaround of prototyping device designs.

3DP offers a number of key advantages over photolithography for mould production. Using photolithographic techniques, structures over 100 μm tall require multiple layers of photoresist to be deposited and baked before patterning and development. Although 3DP also uses the deposition of multiple layers to achieve the same structure, the process is completed in a single automated step.

The structure is designed using 3D computer-aided design (CAD) packages, which is then read directly by the 3DP system. This negates the requirement for photomask production, which may have to be ordered in from third parties. Furthermore, more complex 2.5D structures can be easily produced, as different areas of the moulds can be fabricated to different heights in the same process step, something that would require multiple masks using photolithography. The rapid nature of the process means it is possible to proceed from design conception, via a 3DP mould, to a working PDMS microfluidic chip in around 48 hours.

1.3 Droplet microfluidics

Microfluidic technologies have been demonstrated as a reliable, rapid and high-throughput method for the generation of large numbers of sub-microliter droplets. These techniques have been developed over the past decade to process medical and biological sample for diagnostic and research purposes.[17-19] However, they also hold promise for the production of DIBs.[20] A microfluidic device developed by the de Mello group has demonstrated the production of 2D and 3D arrays of droplets.[21] However, the device was created from an arrangement of plastic tubing, which is not directly compatible with other droplet-based microfluidic techniques that can be integrated using planar chip designs – for example, droplet production was handled off-device using a pipetting robot.

Droplets are normally created in microfluidic chips by flowing an aqueous phase into a continuously-flowing oil phase. The size of the droplets produced is mediated by the ratio of oil to aqueous flow. The device channels are usually hydrophobic in order to minimise aqueous-to-device interaction, either by fabricating the device from a hydrophobic material or by surface treatment. This "continuous" droplet-production approach is useful for the creation of very large numbers of monodisperse droplets, but for smaller droplet network prototypes is difficult to control. Therefore we use a droplet-on-demand technique utilising off-chip solenoid valves that has previously been demonstrated for large-volume droplet production.[22]

Once produced, droplets can subsequently be manipulated into arrays using a number of techniques. Electrowetting is a promising approach, although chip design complexity increases with the need to integrate all but the simplest electrode patterns.[23] It is therefore favourable for the purposes of rapid chip prototyping that droplet manipulation be achieved using passive methods during initial development.

Pillar-mediated droplet merging has been demonstrated as a passive method of temporary microfluidic droplet capture.[24] Several publications in the literature have also outlined the production of surfactant-stabilised linear droplet arrays using pillars. Such arrays have been used for the analysis of droplet-to-droplet compound transport5 and as droplet 'shift registers'.[25] The use of pillars, as opposed to walls, is important as the inter-pillar gaps allow the continuous phase to escape from between the droplets so they can come into contact. It is postulated that the interfaces formed between the droplets is a DIB.

An extension of these techniques is presented here, in order to create simple but configurable linear droplet arrays on-chip with larger droplet numbers. The pillar capture system is augmented by the addition of a 'rail' structure, as shown in *Fig. 2*. This recently developed concept26 uses the reduction in surface energy created by a confined droplet protruding into a trench, fabricated into either the floor or ceiling of a microfluidic chamber. As a result, the droplets are anchored by the rail, but can move along the rail. This allows the production of linear arrays from a wider range of droplet volumes than would be possible with just the pillar-trap structures: smaller droplets would otherwise likely pack into more complex networks than are currently desired.

In this paper we demonstrate the production of linear DIB arrays on-chip, formed from large volume (≥ 1 µl) on-demand droplets for maximised DIB surface area. We then probe the nature of the droplet-droplet interface using melittin, a well-characterised membrane-disrupting peptide. We also demonstrate a novel colorimetric technique for the study of cross-bilayer transport of ions based on the staining of starch by Lugol solution, which also provides evidence of the speed of bilayer formation achieved using this technique.

2. Materials and methods

2.1 Mould preparation

The device was designed using SolidWorks 2011 (Dassault Systemes) and the mould fabricated using a Connex350™ (Objet Geometries) 3D printing (3DP) system. The materials used were VeroWhitePlus™ for the mould structure, deposited on a bed of FullCure®705 support material. Each consecutive layer is deposited using a modified inkjet printer head, heated to 80°C to reduce the prepolymer viscosity, before being cured by an integrated UV lamp. Once fabrication is complete, the support material was removed from underside of the mould using a high-pressure water jet, and the mould dried under stream of compressed air.

Two problems with this technique were identified during initial development. In order to keep material costs low, the moulds were designed to be only 1 mm thick, plus the depth of the fluidic structures. However, these moulds would often warp when removed from the 3DP system. Additionally, it was found that the 3DP surface had an inhibitory effect on the curing of PDMS, via an unknown mechanism. This would leave any PDMS surfaces that were in contact with the mould during curing sticky and unusable.

Both of these problems were overcome by performing an overnight 80°C bake step on the mould. As this is over the glass transition temperature (T_g) of the material (55°C), placing the mould on a glass slide during the bake allowed the material to relax and flatten, without changing the geometry of the mould. The bake step was also found to eliminate the curing inhibition, possibly via the evaporation of the inhibitory agents.

In order to prevent further warping during the baking required to cure PDMS, the mould was adhered to a glass slide. Adhesion was achieved by adding a drop of degassed prepolymer PDMS onto the slide, and placing the mould on top. Baking this mould-PDMS-slide sandwich causes the PDMS to spread and subsequently cure, resulting in a well composite structure that does not warp at higher temperatures. The glass-backed mould was then coated with a layer of trichloro-(1H,1H,2H,2H-perfluorooctyl)silane (Sigma) via vapour deposition for 1 hour at partial pressure in a vacuum desiccator. Although the 3DP material does not bond to PDMS during curing, the glass does stick significantly if the mould is not coated. Mould release directly from the 3DP surface has also been found to be enhanced by the coating procedure.

2.2 PDMS preparation, moulding and bonding

PDMS monomer and curing agent (Sylgard 184, Dow Corning) was mixed at a wt. ratio of 10:1, before being degassed in a vacuum desiccator until no bubbles were visible. The mould was then placed in a foil boat, and the PDMS mixture poured over, giving a device thickness of around 4 mm. The PDMS was then degassed a second time, to remove bubbles formed in the mould structure e.g. the pillars, before being baked at 80°C for 1 hour.

The cured PDMS was then demoulded, and the inlet and outlet holes punched. The PDMS was bonded to a solvent-cleaned 76 x 52 mm glass slide by exposure of both bonding surfaces to oxygen plasma for 30s. The glass and PDMS were manually applied together before being baked for 1 hour at 80°C to allow more complete bonding. Finally, the chip was coated with the same silane material as above, via the same deposition method. This coating makes the glass surface hydrophobic, having been made highly hydrophilic by the plasma treatment, allowing the aqueous droplets produced to move freely inside the chip.

2.3 Device design

The mould design is visualised in *Fig. 3*. The design includes a pair of droplet generators, allowing the production of arrays with droplets of differing compositions. A 'delay line' is included in order to give the lipid time to self-assemble at the fresh aqueous-to-oil interface, a process accelerated by the movement of the aqueous slugs down the microfluidic channel.[27] Finally, a capture chamber, containing both pillar- and rail-based droplet capture structures, was designed to capture droplets of 1 µl and above, which is approximately the range of droplet volumes that are produced reliably by the integrated droplet generators. The microfluidic channels are 1 mm wide and 500 µm deep. The capture pillars are 1,500 x 500 µm in area, separated by 500 µm, and the rail is 300 x 300 µm in profile. The area between the pillar rows is 2 mm across.

2.4 Chip operation and visualisation

Flow through the chip was controlled using syringe pumps (Pump 11 Plus, Harvard Apparatus Ltd., TLC 1000 series syringes, Hamilton Bonaduz AG). For the aqueous solutions, the flow was directly controlled by the syringe pumps alone. The oil flow was spilt off-chip into solenoid valves (LFE series PFE 2-way Micro Inert Valves, The Lee Company) before being introduced to the two droplet generator oil inlets on the chip.

The droplet arrays were monitored using a StereoZoom Discovery (Zeiss) microscope with a Prosilica GC2450C digital camera (Allied Vision Technologies). The image stream was recorded and compiled into video format using custom software, normally set up in a time-lapse mode.

The continuous flow used in these tests was hexadecane (Sigma) with 30 mg/ml dissolved Soy PC (20%) extract (Avanti Polar Lipid). The continuous flow rate was typically used between 50 and 200 µl/min. Hexadecane was used to minimise the material swelling caused by non-polar solvent absorption by the PDMS.

2.5 Membrane disruption by melittin

Melittin (Sigma) was dissolved into buffer (10 mM HEPES, 200 mM KCl) at a concentration of 5 µg/ml. The upper and lower droplet generators were primed with this solution and with plain buffer respectively. A 3 µl droplet of buffer was initially inserted into the array, as the smaller droplets were sometimes found to escape between the end capture pillars. This larger droplet was followed by 6 droplets of 1 µl volume. The linear array formed was topped with a 3 µl droplet of the melittin-containing buffer. The array produced can be seen in *Fig. 4*.

2.6 Colorimetric analysis of droplet interface transport

The device droplet generators were loaded with Lugol solution (Sigma) and 1 % wt. starch solution (Sigma). Lugol solution is a 600 mM KI solution, into which further molecular iodine is dissolved. Non-polar molecular iodine (I_2) does not dissolve in water, but in KI solution it forms KI_3 which is soluble. Triiodide interacts with the amylose form of starch, forming a complex which has a dark blue colour. As shown in *Fig. 5*, linear arrays with alternating droplets of Lugol solution and starch were created and then monitored for colour change.

As it became clear that the iodine was escaping from the droplets into the oil, the oil was saturated with molecular iodine by mixing 10 ml of the Lugol solution with 10 ml of hexadecane for 30 minutes in a rotary mixer. The hexadecane turned purple indicating the presence of dissolved iodine. The oil fraction was then removed from the bottle, and the lipid mixture added, turning the

solution brown/yellow. Further tests, including a control with 600 mM KCl added to the starch droplets, were then carried out to investigate the transfer of ionic species between the droplets, as shown in *Fig. 6*.

3. Results and discussion

3.1 Array formation

Once the chip was primed, aqueous droplets were produced by switching the oil flow to the droplet generator not currently being used. The aqueous column was advanced into the now static oil phase a given volume, extending the column into the oil. The oil flow was then switched back over to the generator in use, pinching off the slug into a slug of the volume desired. This technique allows the production of larger droplets than would otherwise be possible, as the larger slugs would be broken into smaller droplets by a continuous oil flow.

Once produced, the droplets flow through the delay line and into the capture chamber. Droplet movement is maintained due to the continuous oil flow. The swapping of the continuous flow between the two droplet generators reduces the effect of droplet production on the downstream microfluidic elements, allowing the oil flow to remain relatively constant. As shown in *Fig. 2*, the first droplet into the array is captured by the shaped end pillars. Further droplets are forced into contact with previously trapped droplets. Higher flow rates were found to produce arrays with flatter, larger-area droplet-to-droplet interfaces. Without the continuous flow to hold them together, the droplets will return to a more rounded shape, and if the chip is not levelled correctly may float apart.

Droplet arrays produced with mild aqueous solution were found to be stable over extended periods of time, and were monitored for up to 6 hours. The practical limiting factors in array duration were the requirement for a continuous oil phase supply, and the swelling effect induced by the oil phase absorbing into the PDMS,[28] which eventually causes the chamber ceiling to be forced upwards breaking the array. However, this effect was more pronounced in initial experiments using decane as the continuous phase rather than hexadecane.

After the linear arrays had been observed, the chip was cleared for the next set of droplets by manually compressing the array chamber, expelling the droplets from between the pillars. It was found that substantially increasing the continuous flow (1,000-2,000 µl/min) accelerated this process.

3.2 Melittin disruption of DIBs

The array seen in *Fig. 4* is not initially completely linear. However, the rail has held the droplets sufficiently that each of the droplets only contacts with one droplet on each size. As the larger, melittin-containing droplet merges with the smaller droplets, the effect on the surface tension by melittin is evident as it starts to flow around the other droplets due to the force exerted by the continuous oil flow.

Despite this, the array lasted long enough to show the effect of the melittin on DIB stability. At the relatively high concentration used, the larger peptide-containing droplet merged sequentially with the otherwise stable buffer-containing droplets. As expected, the time delay between merging events increases as the melittin is diluted by the buffer from droplets it has consumed. This is seen as an indication that the droplet-to-droplet interface is free of the continuous phase and is in fact a DIB, as the melittin would in this situation have no effect on the stability of the droplet array.

3.3 Iodine/starch for analysis of ionic transfer across DIBs

The iodine-starch test allows the detection of starch with a solution containing dissolved molecular iodine, or vice versa. Diatomic iodine is non-polar and is not normally soluble in water. However, if an aqueous solution contains ionic potassium iodide (KI) the molecular iodine complexes with the KI to form water-soluble potassium triiodide (KI_3). The triiodide ion subsequently complexes with the helical amylose component of the starch, which forms a deep blue colour due to the alignment of the triiodide ions.

As would be expected, the large difference in ionic strength between the contacted droplets, containing Lugol's iodine (I_2 saturated KI solution) and starch respectively, caused the translocation of the KI_3 across the droplet-droplet interface. Within a few seconds the triiodide-starch complex is visible within the starch droplet, towards the droplet edge as shown in *Fig. 5*. The effect of this ionic transfer is enough to eventually cause the bilayer to break, allowing the droplets to merge. Should any continuous phase be present between the droplet-interface monolayers, this effect would not be seen as the ionic KI_3 is not soluble in the oil phase.

However, the escape of what is assumed to be molecular iodine from the droplets into the oil phase was noticed early during testing. It is assumed that the KI_3 disassociates into KI and I_2, the latter of which is non-polar and can dissolve into the hexadecane. A practical effect of this loss is that the arrays must be formed quickly, in order to reduce iodine loss from the droplets and maximise the colorimetric signal. Once in the arrays, the droplets are shielded from the oil flow by the pillars, reducing iodine diffusion.

In order to reduce the loss of iodine, the oil phase was saturated with molecular iodine. Control tests were then carried out on arrays with droplets containing just the starch solution and droplets with starch and 600 mM KCl. Interestingly, the starch-only linear array remained stable over a period of 30 minutes. However, the KCl containing droplets formed patches of blue staining. This shows that the presence of potassium ions is required as a counter-ion for the formation of the triiodide ions required for the staining of starch.

This behaviour is further indicative of the formation of DIBs between the droplets in the array. It would be possible if an oil layer was present between the droplet monolayers that the staining could be due to the molecular iodine crossing the oil gap. However, the fact that staining does not occur without a counter ionic species shows that the KI_3 is the ionic species cross the bilayer, which would not happen if a non-polar oil layer was present, as outlined in *Fig. 7*.

4. Conclusions

We have presented a microfluidic chip that allows the production of large-volume droplets, and their controlled arrangement into linear DIB arrays. The nature of the inter-droplet interfaces has been confirmed as a bilayer, both by the observed droplet destabilisation by melittin, and using a novel method that visualises the ionic transport of KI_3 across the bilayer via the staining of starch. The development of the device was accelerated by the use of a 3DP system to produce the moulds, allowing a 48 hour design conception to chip testing turnaround.

It is hoped such devices will allow the further development of large DIB arrays in a rapid, automated fashion that does not require the same level of manual intervention as conventional techniques. This device could be modified in future to produce branching arrays. A final observation can be made on how well previously demonstrated microdroplet techniques, such as flow-focussing,

droplets-on-rails and pillar-mediate droplet trapping, scale to such large droplet volumes without requiring any further modification other than the increase in feature size.

5. Acknowledgements

The research reported here is supported in part by Future and Emerging Technologies Grant FP7-248992 “NEUNEU” from the European Union.

6. References

1. L. M. Tsofina, E. A. Liberman and A. V. Babakov, Nature, 1966, 212, 681-683.
2. H. Bayley, B. Cronin, A. Heron, M. A. Holden, W. L. Hwang, R. Syeda, J. Thompson and M. Wallace, Mol Biosyst, 2008, 4, 1191-1208.
3. R. Syeda, M. A. Holden, W. L. Hwang and H. Bayley, J Am Chem Soc, 2008, 130, 15543-15548.
4. S. Aghdaei, M. E. Sandison, M. Zagnoni, N. G. Green and H. Morgan, Lab Chip, 2008, 8, 1617-1620.
5. Y. P. Bai, X. M. He, D. S. Liu, S. N. Patil, D. Bratton, A. Huebner, F. Hollfelder, C. Abell and W. T. S. Huck, Lab Chip, 2010, 10, 1281-1285.
6. M. R. R. de Planque, S. Aghdaei, T. Roose and H. Morgan, Acs Nano, 2011, 5, 3599-3606.
7. K. Funakoshi, H. Suzuki and S. Takeuchi, Analytical Chemistry, 2006, 78, 8169-8174.
8. N. Malmstadt, M. A. Nash, R. F. Purnell and J. J. Schmidt, Nano Lett, 2006, 6, 1961-1965.
9. M. A. Holden, D. Needham and H. Bayley, J Am Chem Soc, 2007, 129, 8650-8655.
10. W. L. Hwang, M. A. Holden, S. White and H. Bayley, J Am Chem Soc, 2007, 129, 11854-11864.
11. G. Villar, A. J. Heron and H. Bayley, Nat Nano, 2011, 6, 803-808.
12. Y. Xia and G. M. Whitesides, Annual Review of Materials Science, 1998, 28, 153-184.
13. M. A. Unger, H.-P. Chou, T. Thorsen, A. Scherer and S. R. Quake, Science, 2000, 288, 113-116.
14. K. Haubert, T. Drier and D. Beebe, Lab Chip, 2006, 6.
15. M. C. Huang, H. Ye, Y. K. Kuan, M. H. Li and J. Y. Ying, Lab Chip, 2009, 9, 276-285.
16. A. Bonyar, H. Santha, B. Ring, M. Varga, J. G. Kovacs and G. Harsanyi, Procedia Engineer, 2010, 5, 291-294.
17. G. F. Christopher and S. L. Anna, J Phys D Appl Phys, 2007, 40, R319-R336.
18. A. Huebner, S. Sharma, M. Srisa-Art, F. Hollfelder, J. B. Edel and A. J. Demello, Lab Chip, 2008, 8, 1244-1254.
19. S. Y. Teh, R. Lin, L. H. Hung and A. P. Lee, Lab Chip, 2008, 8, 198-220.
20. M. Zagnoni, Lab Chip, 2012.
21. C. E. Stanley, K. S. Elvira, X. Z. Niu, A. D. Gee, O. Ces, J. B. Edel and A. J. deMello, Chem Commun, 2010, 46, 1620-1622.
22. K. Churski, P. Korczyk and P. Garstecki, Lab Chip, 2010, 10, 816-818.
23. F. Malloggi, H. Gu, A. Banpurkar, S. Vanapalli and F. Mugele, The European Physical Journal E: Soft Matter and Biological Physics, 2008, 26, 91-96.
24. X. Niu, S. Gulati, J. B. Edel and A. J. deMello, Lab Chip, 2008, 8, 1837-1841.
25. M. Zagnoni and J. M. Cooper, Lab Chip, 2010, 10, 3069-3073.
26. P. Abbyad, R. Dangla, A. Alexandrou and C. N. Baroud, Lab Chip, 2011, 11.
27. J. C. Baret, F. Kleinschmidt, A. El Harrak and A. D. Griffiths, Langmuir, 2009, 25, 6088-6093.
28. J. N. Lee, C. Park and G. M. Whitesides, Analytical Chemistry, 2003, 75, 6544-6554.

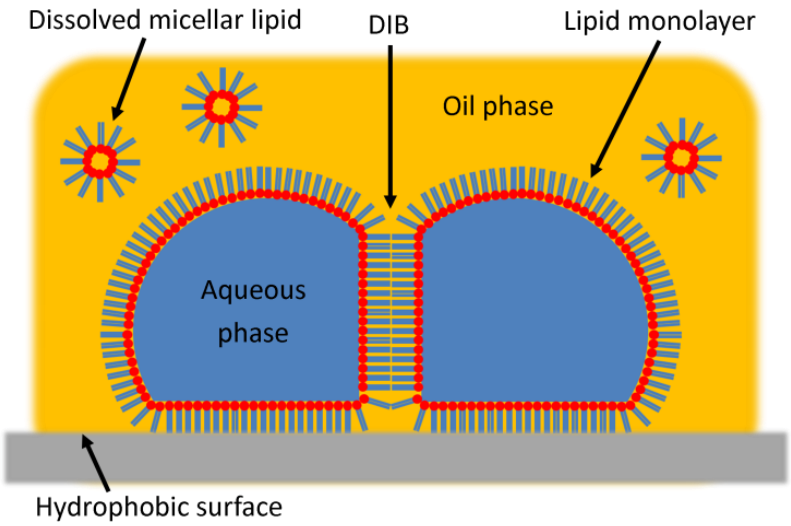

Fig. 1 *The concept of droplet interface bilayers (DIBs) in lipid-out configuration (lipid dissolved in oil).*

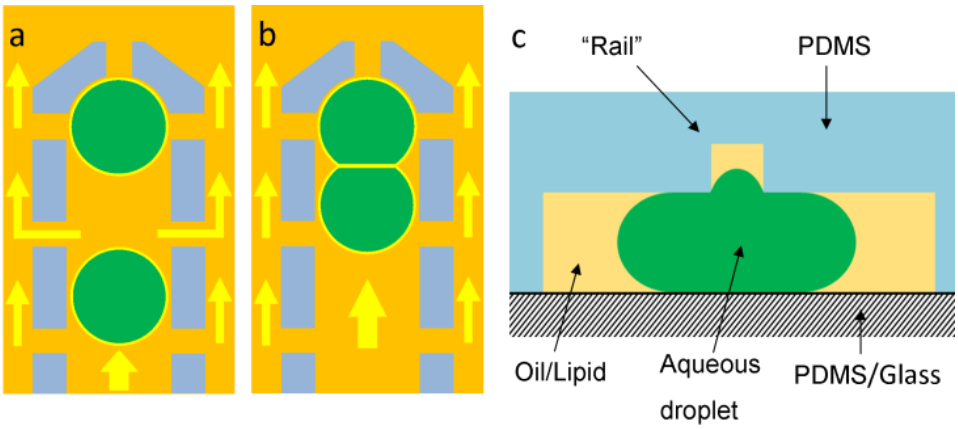

Fig. 2 *Pillar- and rail-mediated linear droplet array formation. Droplets are carried by the lipid-in-oil flow (yellow arrows) into the capture chamber (a). Subsequent droplets stack up against those that have previously entered (b). Oil trapped between the droplets can escape between the pillars, allowing the droplets to come into contact. Smaller droplets are prevented from packing in non-linear arrays by the presence of the rail (c), forming smaller area DIBs.*

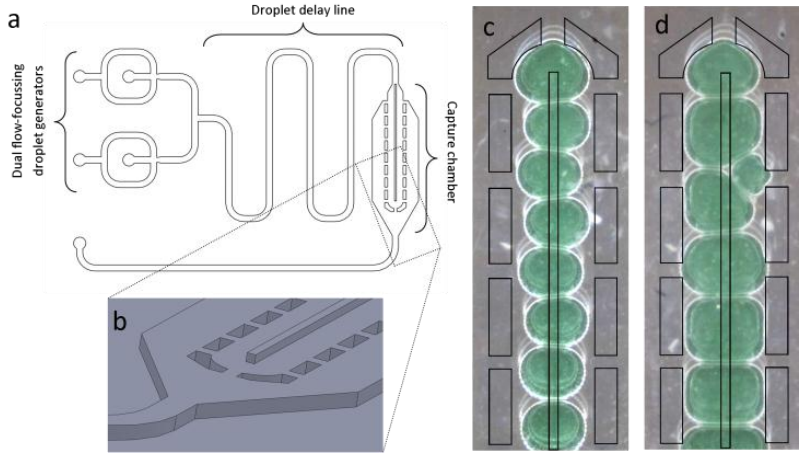

Fig. 3 *Microfluidic chip design for on-chip droplet production and capture, with resulting arrays. 2D (a) and 3D (b) CAD representations of the mould design are shown, highlighting the rail feature, which is fabricated directly during the 3DP process. Arrays of aqueous droplets containing food dye are shown, both in rail-mediated (c) and pillar-mediated forms (d).*

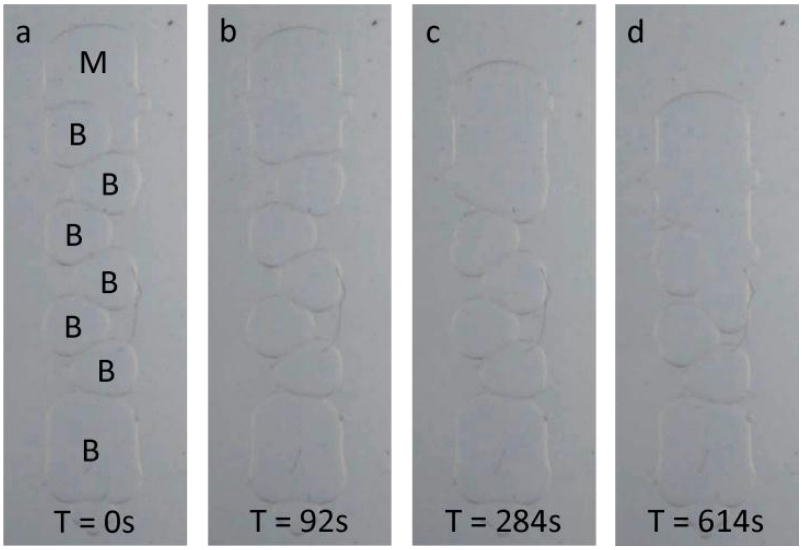

Fig. 4 *Destruction of DIBs by melittin. A linear array of droplets is set up as described in the text. The initial array is shown, composed of buffer- (B) and melittin-containing (M) droplets (a). The melittin-containing droplet proceeds to merge with the buffer droplets (b-d).*

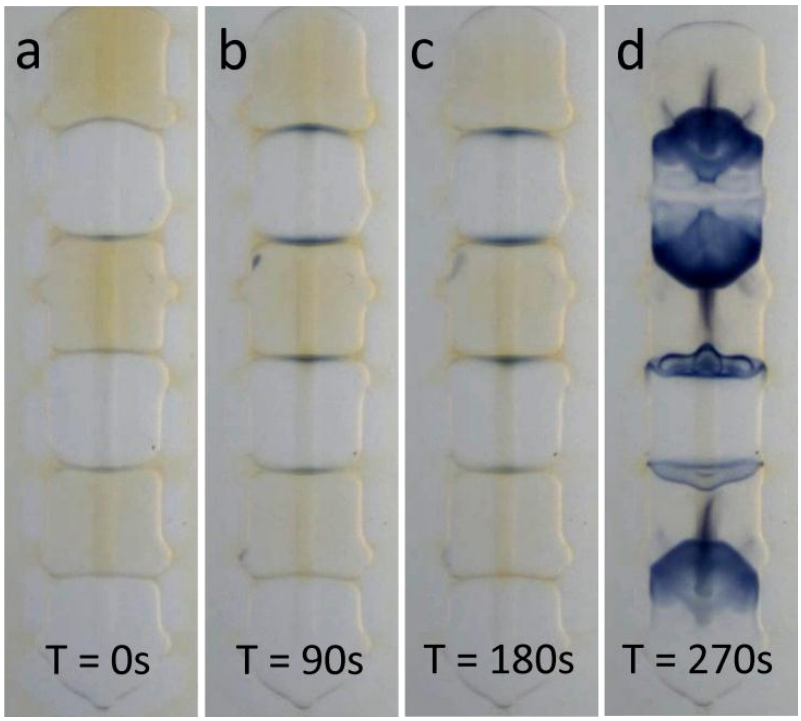

Fig. 5 *Transport of ionic species across a DIB, driven by a high concentration gradient. Upon initial array formation very little staining is evident (a). However, over time (b, c) the staining at the starch droplet interface becomes darker. After a few minutes, the bilayers are destroyed by the ionic flux (d).*

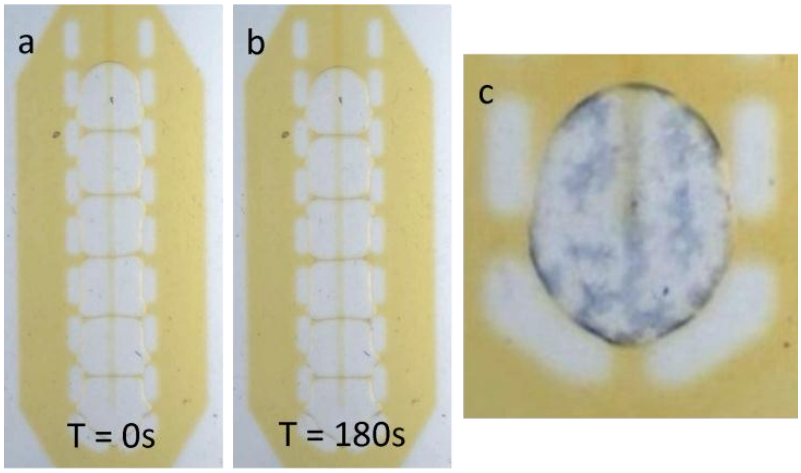

Fig. 6 *The effect of saturation of the continuous phase with iodine. Arrays produced with 3 µl droplets containing only the starch solution were found to be stable over extended periods, in comparison to mixed iodine/starch droplet arrays (a, b). However, the addition of 600 mM KCl to the droplets produced staining (c).*

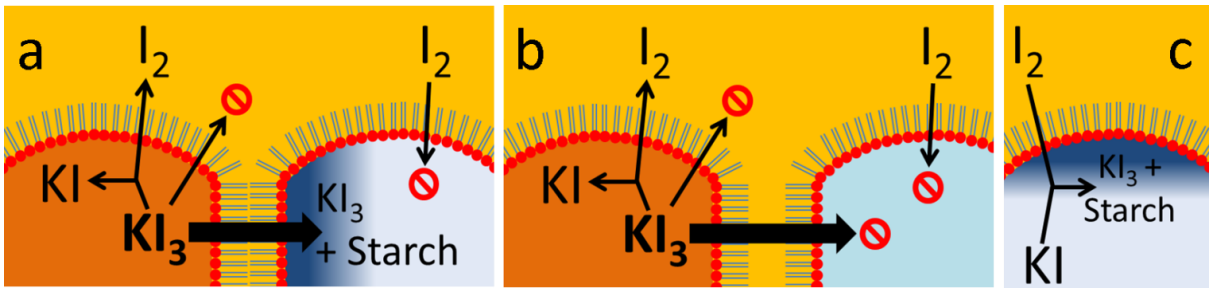

Fig. 6 *Ionic and non-ionic transport observed during testing. When a DIB is formed between a droplet containing KI_3 and another containing starch, the KI_3 is forced across the bilayer by the high ionic concentration gradient. I_2 also escapes the droplet into the non-polar oil phase, having disassociated from the KI_3, leaving KI dissolved in the solution. However, the I_2 cannot enter the starch droplet, due to the lack of a positive counter-ion (a). If an oil layer was present between the droplet interface monolayers, the transport of KI_3 would be blocked, as it is ionic and insoluble in the non-polar continuous phase (b). However, if KCl is added to the starch, the molecular iodine can diffuse across the membrane and form KI_3, producing the starch-KI_3 complex (c).*